

1 Modulation of pulsatile GnRH 2 dynamics across the ovarian cycle: 3 the role of glutamatergic transmission 4 in the arcuate kisspeptin network.

5
6 Margaritis Voliotis^{1,*†}, Xiao Feng Li^{2,†}, Ross De Burgh^{2,†}, Geffen Lass², Deyana Ivanova²,
7 Caitlin McIntyre², Kevin T. O’Byrne^{2,*}, Krasimira Tsaneva-Atanasova^{1,*}
8 ¹Department of Mathematics and Living Systems Institute, College of Engineering,
9 Mathematics and Physical Sciences, University of Exeter, Exeter, EX4 4QF, UK.
10 ²Department of Women and Children’s Health, School of Life Course Sciences, King’s
11 College London, London SE1 1UL, UK.
12 [†] These authors contributed equally to this work
13 ^{*} For correspondence: M.Voliotis@exeter.ac.uk, Kevin.O’Byrne@kcl.ac.uk, K.Tsaneva-
14 Atanasova@exeter.ac.uk

15

16 **Abstract**

17 Pulsatile GnRH release is essential for normal reproductive function. Kisspeptin secreting
18 neurons found in the arcuate nucleus, known as KNDy neurons for co-expressing neurokinin
19 B, and dynorphin, drive pulsatile GnRH release. Furthermore, gonadal steroids regulate
20 GnRH pulsatile dynamics across the ovarian cycle by altering KNDy neurons' signalling
21 properties. However, the precise mechanism of regulation remains mostly unknown. To
22 better understand these mechanisms we start by perturbing the KNDy system at different
23 stages of the estrous cycle using optogenetics. We find that optogenetic stimulation of KNDy
24 neurons stimulates pulsatile GnRH/LH secretion in estrous mice but inhibits it in diestrous
25 mice. These in-vivo results in combination with mathematical modelling suggest that the
26 transition between estrus and diestrus is underpinned by well-orchestrated changes in
27 neuropeptide signalling and in the excitability of the KNDy population controlled via
28 glutamate signalling. Guided by model predictions, we show that blocking glutamate
29 signalling in diestrous animals inhibits LH pulses, and that optic stimulation of the KNDy
30 population mitigates this inhibition. In estrous mice, disruption of glutamate signalling
31 inhibits pulses generated via sustained low-frequency optic stimulation of the KNDy
32 population, supporting the idea that the level of network excitability is critical for pulse

33 generation. Our results reconcile previous puzzling findings regarding the estradiol-
34 dependent effect that several neuromodulators have on the GnRH pulse generator dynamics.
35 Therefore, we anticipate our model to be a cornerstone for a more quantitative understanding
36 of the pathways via which gonadal steroids regulate GnRH pulse generator dynamics.
37 Finally, our results could inform useful repurposing of drugs targeting the glutamate system
38 in reproductive therapy.

39 **Introduction**

40 The dynamics of gonadotropin-releasing hormone (GnRH) secretion is critical for
41 reproductive health. In female animals, GnRH secretion is tightly regulated across the
42 ovarian cycle. Pulsatile secretion dominates most of the cycle, with frequency and amplitude
43 modulated by the ovarian steroid feedback. Positive feedback from increasing estradiol levels
44 triggers a preovulatory surge of GnRH/LH secretion (Christian and Moenter, 2010).
45 Furthermore, there is ample evidence that ARC kisspeptin neurons are prime mediators of the
46 ovarian steroid feedback on the pulsatile dynamics of GnRH/LH secretion (McQuillan et al.,
47 2019), although the mechanisms remain unclear.

48 *In-vitro* studies have shown that gonadal steroids have a dramatic effect on the
49 electrophysiology of ARC kisspeptin neurons. For instance, spontaneous firing activity of
50 ARC kisspeptin neurons from castrated mice appears elevated compared to intact animals
51 (Ruka et al., 2016) and estradiol replacement attenuates ARC kisspeptin neuron activity in
52 gonadectomised animals (Ruka et al., 2016; Wang et al., 2018). More recently, fiber
53 photometry data from female mice show that the ARC kisspeptin neuronal population
54 (KNDy network) pulses at a relatively constant frequency throughout the ovarian cycle apart
55 from the estrous phase where the frequency is dramatically reduced (McQuillan et al., 2019).
56 This silencing effect is thought to be a direct consequence of the increasing progesterone
57 levels in the circulation associated with ovulation (McQuillan et al., 2019). Furthermore,
58 studies in the sheep indicate the silencing effect of progesterone is mediated through
59 increased dynorphin signalling (Goodman et al., 2011; Moore et al., 2018), however this is
60 less clear in mice where ovarian steroids have a negative effect on Dyn mRNA levels
61 (Navarro et al., 2009).

62 Perplexing is also the differential effect of various neuromodulators on LH secretion
63 depending on the gonadal steroid background. For instance, N-methyl-D-aspartate (NMDA)
64 robustly inhibits LH pulses in the ovariectomized monkey whereas in the presence of

65 estradiol this effect is reversed, and NMDA stimulates LH secretion (Reyes et al., 1990;
66 Reyes et al., 1991). Similar reversal of action on LH dynamics depending on the underlying
67 ovarian steroid milieu has been also documented for other neurotransmitter and
68 neuropeptides in other species (Kalra and Kalra, 1983; Brann and Mahesh, 1992; Arias et al.,
69 1993; Bonavera et al., 1994; Scorticati et al., 2004) and highlights the complex mechanisms
70 underlying the modulation the GnRH pulse generator by gonadal steroids.

71 Here, using mathematical modelling along with optogenetic stimulation of ARC kisspeptin
72 neurons we embark to understand how the dynamics of the pulse generator are modulated
73 across the ovarian cycle. Our mathematical model suggests that the level of excitability
74 within the ARC kisspeptin network—the propensity of kisspeptin neurons to signal and
75 activate each other—is one of the key parameters modulated in different stages of the cycle
76 by gonadal steroids. Previous studies have shown that ARC kisspeptin neurons synapse on
77 each other (Yip et al., 2015; Qiu et al., 2016) and are glutamatergic (Cravo et al., 2011; Qiu
78 et al., 2011; Kelly et al., 2013; Nestor et al., 2016; Qiu et al., 2016; Wang et al., 2018). Based
79 on these findings we hypothesise that population excitability should be enabled primarily via
80 glutamate signalling. We test our predictions *in-vivo* and show that glutamatergic
81 transmission is an important factor for the pulsatile behaviour of the KNDy network.

82 **Materials and methods**

83 **Animals**

84 Adult Kiss-Cre heterozygous transgenic female mice aged between 8-14 weeks, 25-30 g,
85 were used for experiments (Yeo et al., 2016). Breeding pairs were obtained from the
86 Department of Physiology, Development and Neuroscience, University of Cambridge, UK
87 and mated in house at King's College London. Genotyping was performed using a multiplex
88 PCR protocol for detection of heterozygosity for the Kiss-Cre or wild-type allele as
89 previously described (Lass et al., 2020). Only mice with normal estrous cycles were used.
90 Daily vaginal smears were performed for the detection of the estrous and diestrous stages of
91 the ovarian cycle. Mice were singularly housed and provided with food (standard
92 maintenance diet; Special Dietary Services, Wittam, UK) and water ad libitum while being
93 kept under a 12:12 h light/dark cycle (lights on 0700 h) at $23 \pm 2^\circ\text{C}$. All animal procedures
94 performed were approved by the Animal Welfare and Ethical Review Body Committee at
95 King's College London and conducted in accordance with the UK Home Office Regulations.

96 **Surgical procedures**

97 Stereotaxic injection of AAV9-EF1-dflox-hChR2-(H134R)-mCherry-WPRE-hGH (4.35 x
98 10¹³ GC/ml; Penn Vector Core; University of Pennsylvania, PA, USA) for targeted
99 expression of channelrhodopsin (ChR2) in ARC kisspeptin neurons was done under aseptic
100 conditions. The mice were anaesthetised using ketamine (Vetalar, 100 mg/kg, i.p.; Pfizer,
101 New York City, NY, USA) and xylazine (Rompun, 10 mg/kg, i.p.; Bayer, Leverkusen,
102 Germany). Kiss-Cre female mice (n = 12) or wilt-type (n = 3) were secured in a Kopf
103 Instruments motorized stereotaxic frame (Kopf Instruments, Tujunga, CA, USA) and surgical
104 procedures on the brain were performed using a Robot Stereotaxy system (Neurostar,
105 Tübingen, Germany). Stereotaxic injection coordinates used to target the ARC were obtained
106 from the mouse brain atlas of Paxinos and Franklin (Paxinos and Franklin, 2004) (0.25 mm
107 lateral, 1.94 mm posterior to bregma and at a depth of 5.8 mm). A skin incision was made
108 and a small hole was drilled in the skull above the location of the ARC. A 2- μ l Hamilton
109 micro-syringe (Esslab, Essex, UK) was attached to the robot stereotaxy and used to inject
110 0.3 μ l of the AAV-construct into the ARC, unilaterally, at a rate of 100 nl/min. After the
111 injection, the needle was left in position for 5 min and then slowly lifted over 1 min. The
112 same coordinates as the injection site were then used to insert a fiber-optic cannula (200 μ m,
113 0.39 NA, 1.25 mm ceramic ferrule; Thorlabs, LTD, Ely, UK), however a depth of 5.78 mm
114 was reached to ensure the fiber-optic cannula was situated immediately above the injection
115 site. Additionally, an intracerebroventricular (ICV) fluid guide cannulae (26 gauge; Plastics
116 One) targeting the lateral ventricle (coordinates: 1.1 mm lateral, 1.0 mm posterior to bregma
117 and at a depth of 3.0 mm) was chronically implanted. Dental cement (Superbond C&B kit
118 Prestige Dental Products, Bradford UK) was used to fix the cannulae in place and the skin
119 incision was sutured. A one week recovery period was given post-surgery. After this period,
120 the mice were handled daily to acclimatize them to the tail-tip blood sampling procedure
121 (Steyn et al., 2013). Mice were left for 4 weeks to achieve effective opsin expression before
122 experimentation.

123 **Validation of AAV injection site and fibre optic and ICV cannula position**

124 Once experiments were completed, mice were given a lethal dose of ketamine and
125 transcardially perfused for 5 min with heparinized saline, followed by 10 min of ice-cold 4%
126 paraformaldehyde (PFA) in phosphate buffer, pH 7.4, for 15 min using a pump (Minipuls;
127 Gilson). Brains were collected immediately and post fixed at 4°C in 15% sucrose in 4% PFA
128 and left to sink. They were then transferred to 30% sucrose in PBS until they sank. The brains

129 were then snap-frozen on dry ice and stored at -80°C . Using a cryostat, every third coronal
130 brain section ($30\ \mu\text{m}$) was collected between $-1.34\ \text{mm}$ to $-2.70\ \text{mm}$ from bregma and
131 sections were mounted on microscope slides, left to air-dry and cover slipped with ProLong
132 Antifade mounting medium (Molecular Probes, Inc, OR, USA). Verification and evaluation
133 of the injection site was performed using an Axioskop 2 Plus microscope equipped with
134 axiovision 4.7 (Zeiss). One of 12 Kiss-Cre mice failed to show mCherry fluorescence in the
135 ARC and was excluded from the analysis.

136 **Experimental design and blood sampling for LH measurement.**

137 For measurement of LH pulsatility during optogenetic stimulation, the tip of the mouse's tail
138 was removed with a sterile scalpel for tail-tip blood sampling (Czieselsky et al., 2016). The
139 chronically implanted fiber-optic cannula was attached to a multimode fiber-optic rotary joint
140 patch cables (Thorlabs) via a ceramic mating sleeve. This allows for freedom of movement
141 and blue light delivery ($473\ \text{nm}$ wavelength) using a Grass SD9B stimulator controlled DPSS
142 laser (Laserglow Technologies) during optogenetic stimulation.

143 The experimental protocol involved an hour long acclimatisation period, followed by 2.5 h of
144 blood sampling, where $5\ \mu\text{l}$ of blood was collected every 5 min. For estrous and diestrous
145 mice, optic stimulation was initiated after 1 h of control blood sampling and was sustained
146 for 1.5 h. Optic stimulation was delivered as 5ms pulses of light at 5 Hz with the laser
147 intensity measured at the tip of the fiber-optic patch cable set to 5mW (Voliotis et al., 2019).
148 Additionally, in separate experiments, diestrous mice were optically stimulated at 5 or 15 Hz
149 for 2.5 h, that is entire blood sampling period. Control mice (in estrus or diestrus) received no
150 optic stimulation. Wild-type mice (estrus and diestrus) received 5 Hz optic stimulation to
151 verify that our optic stimulation protocol had no undesirable effects on LH secretion.

152 Neuropharmacological manipulation of glutamatergic signalling was performed using a
153 combination of NMDA (AP5, Tocris, Abingdon, UK) and AMPA (CNQX, Alpha Aesar,
154 Heysham, UK) receptor antagonist treatment with or without simultaneous optogenetic
155 stimulation. The animals were prepared for optogenetic experimentation as described above
156 with additional preparation of the ICV injection cannula. Immediately after connection of the
157 fiber-optic cannula, the ICV injection cannula with extension tubing, preloaded with drug
158 solution (AP5 and CNQX dissolved in artificial CSF) or artificial CSF alone as control, was
159 inserted into the guide cannula. The extension tubing, reaching outside of the cage, was
160 connected to a $10\ \mu\text{l}$ Hamilton syringe mounted in an automated pump (Harvard Apparatus)
161 to allow for remote micro-infusion without disturbing the animals during experimentation.

162 After a 55 min control blood sampling period, as described above, and 5 min before the onset
163 of optic stimulation, a bolus ICV injection of drug solution (12 nmol AP5 and 5 nmol CNQX
164 in 2.3 μ l) was given over 5 min, followed by a continuous infusion (20 nmol AP5 and 10
165 nmol CNQX in 5.6 μ l) for the remaining 90 min of experimentation. Artificial CSF controls,
166 with or without optic stimulation, received the same ICV fluid regime. When no optic
167 stimulation was applied the same ICV administration and blood sampling regimen described
168 was applied. Stimulation and non-stimulation protocols were implemented in random order
169 for Kiss-Cre mice.

170 The blood samples were snap-frozen on dry ice and stored at -80°C until processed. In-house
171 LH enzyme-linked immunosorbent assay (LH ELISA) similar to that described by Steyn et
172 al. was used for processing of the mouse blood samples (Steyn et al., 2013). The mouse LH
173 standard (AFP- 5306A; NIDDK-NHPP) was purchased from Harbor-UCLA along with the
174 primary antibody (polyclonal antibody, rabbit LH antiserum, AFP240580Rb; NIDDK-
175 NHPP). The secondary antibody (donkey anti-rabbit IgG polyclonal antibody [horseradish
176 peroxidase]; NA934) was from VWR International. Validation of the LH ELISA was done in
177 accordance with the procedure described in Steyn et al. (Steyn et al., 2013) derived from
178 protocols defined by the International Union of Pure and Applied Chemistry. Serially diluted
179 mLH standard replicates were used to determine the linear detection range. Nonlinear
180 regression analysis was performed using serially diluted mLH standards of known
181 concentration to create a standard curve for interpolate the LH concentration in whole blood
182 samples, as described previously (Voliotis et al., 2019). The intraassay and interassay
183 variations were 4.6% and 10.2%, respectively.

184 **LH pulse detection and statistical analysis.**

185 Dynpeak algorithm was used for the detection of LH pulses (Vidal et al., 2012). The
186 differential effect of optogenetic stimulation on LH pulsatility in estrus and diestrus was
187 determined by looking at the frequency of LH pulses. For mice in estrus and for the
188 neuropharmacological experiments, the mean \pm SEM of LH pulses per hour were compared
189 between the 60 min pre-stimulation/drug delivery control period and subsequent 90 min
190 stimulation period. For mice in diestrus, the mean \pm SEM of LH pulses per hour were
191 compared between controls, 5 Hz and 15 Hz treatment groups, as optic stimulation was
192 applied from the beginning of blood sample period. No optic stimulation was applied to
193 control animals, however the same time points were compared. The frequency of LH pulses
194 in the 90-min optic stimulation/drug delivery period was also compared between treatment

195 groups. One-way ANOVA followed by Dunnett's test, $p < 0.05$, was used to determine
 196 statistical significance.

197 **Mathematical model of the KNDy network.**

198 We used a modified version of our previously published mathematical model of the KNDy
 199 network (Voliotis et al., 2019). Briefly, the model describes the ARC kisspeptin population in
 200 terms of three variables: \bar{D} , the average concentration of Dyn secreted by the population; \bar{N} ,
 201 the average concentration of NKB secreted by the population; and \bar{v} , the average firing
 202 activity of the population, measured in spikes/min. The variables obey the following set of
 203 coupled ordinary differential equations (ODEs):

$$\frac{d\bar{D}}{dt} = f_D(\bar{v}) - d_D\bar{D}; \quad [1]$$

$$\frac{d\bar{N}}{dt} = f_N(\bar{v}, \bar{D}) - d_N\bar{N}; \quad [2]$$

$$\frac{d\bar{v}}{dt} = f_v(\bar{v}, \bar{N}) - d_v\bar{v}. \quad [3]$$

204

205 Parameters d_D , d_N and d_v control the characteristic timescale of each variable. The secretion
 206 rate of Dyn and NKB are given by:

$$f_D(\bar{v}) = k_{D,0} \frac{\bar{v}^{n_1}}{\bar{v}^{n_1} + K_{v,1}^{n_1}};$$

$$f_N(\bar{v}, \bar{D}) = k_N \frac{\bar{v}^{n_2}}{\bar{v}^{n_2} + K_{v,2}^{n_2}} \frac{K_D^{n_3}}{\bar{D}^{n_3} + K_D^{n_3}}.$$

207 In the equations above neuronal activity (\bar{v}) stimulates secretion of both neuropeptides, and
 208 Dyn represses NKB secretion. The maximum secretion rate for the two neuropeptides is
 209 controlled by parameters k_D and k_N and we refer to these parameters as the strength of Dyn
 210 and NKB signalling respectively. The effector levels at which saturation occurs are controlled
 211 via parameters $K_{v,1}$, $K_{v,2}$ and K_D . Here, we are interested in investigating the effect of
 212 network excitability on the dynamics therefore we modify the equation for the neuronal
 213 activity, \bar{v} , by setting:

$$214 \quad f_v(\bar{v}, \bar{N}) = v_0 \frac{1 - \exp(-I)}{1 + \exp(-I)}; I = I_0 + k_v \left(\frac{N^{n_4}}{N^{n_4} + K_N^{n_4}} \bar{v} \right),$$

215 where we have introduced parameter k_v capturing the strength of the synaptic connections
 216 between KNDy neurons in the ARC and which we will use as a proxy for intrinsic network
 217 excitability. Furthermore, v_0 is the maximum rate at which the firing rate increases in

218 response to synaptic inputs I . Note the stimulatory effect of NKB (which is secreted at the
 219 presynaptic terminal) on neuronal activity (Qiu et al., 2016). Finally, parameter I_0 controls
 220 the basal neuronal activity in the population, which could stem from synaptic noise or
 221 afferent inputs. Table 1 give the full list of model parameters.

222

223 **Parameter inference**

224 We used Approximate Bayesian Computation (ABC) based on sequential Monte Carlo
 225 (SMC) (Toni et al., 2009) to infer four key model parameters (Dyn signalling strength, k_D ;
 226 NKB signalling strength, k_N ; network excitability k_v ; and basal activity, I_0) in the estrous
 227 and diestrous phase of the ovarian cycle. For this inference we used the average LH pulse
 228 frequency observed in four different settings: estrous animals without optic stimulation (F_E)
 229 and with 5Hz optic stimulation (F_{E+5Hz}); diestrus animals without optic stimulation (F_D) and
 230 with 5Hz optic stimulation (F_{D+5Hz}). Model simulations were generated in Matlab using
 231 function ode45 under the four different settings for 6000min and by calculating the
 232 frequencies after discarding the initial 1000min. The following discrepancy function was
 233 used to compare simulated, $D^* = (F_E^*, F_{E+5Hz}^*, F_D^*, F_{D+5Hz}^*)$, and experimental, $D =$
 234 $(F_E, F_{E+5Hz}, F_D, F_{D+5Hz})$, data:

$$d(D, D^*) = \max(\text{abs}(D - D^*))$$

235 Furthermore, for the ABC SMC algorithm the size of the particle population was set to 500
 236 and the algorithm was run for $T = 4$ populations with corresponding tolerance levels
 237 $\varepsilon_i = 10^{2-i}, i = 1, \dots, T$. Prior distributions were formulated in the logarithmic space to
 238 explore the behavior of the model under a wide range of parameter values:
 239 $\log_{10}(k_D) \sim \text{Uniform}(-3, 3)$, $\log_{10}(k_N) \sim \text{Uniform}(-3, 3)$, $\log_{10}(k_v) \sim \text{Uniform}(-3, 3)$.,
 240 $\log_{10}(I_0) \sim \text{Uniform}(-3, 3)$. All remaining parameters were fixed to values found in the
 241 literature (see Table 1). For each parameter an independent \log_{10} -normal perturbation kernel
 242 with variance 0.05 was used.

No	Parameter	Description	Value	Ref.
1	d_D	Dyn degradation rate	0.25 min^{-1}	(Voliotis et al., 2019)
2	d_N	NKB degradation rate	0.25 min^{-1}	(Voliotis et al., 2019)
3	d_v	Firing rate reset rate	10 min^{-1}	(Qiu et al., 2016)
4	k_D	Dyn signalling strength	inferred	
5	k_N	NKB signalling strength	inferred	(Ruka et al., 2016)
6	k_v	Network excitability	inferred	
7	v_0	Maximum rate of neuronal activity increase	$30000 \text{ spikes min}^{-2}$	(Qiu et al., 2016)
8	K_D	Dyn IC_{50}	0.3 nM	(Yasuda et al., 1993)

9	K_N	NKB EC_{50}	32 nM	(Seabrook et al., 1995)
10	$K_{v,1}$	Firing rate for half-maximal Dyn secretion	1200 spikes min^{-1}	(Dutton and Dyball, 1979)
11	$K_{v,2}$	Firing rate for half-maximal NKB secretion	1200 spikes min^{-1}	(Dutton and Dyball, 1979)
12	I_0	Basal activity	inferred	
13	n_1, n_2, n_3, n_4	Hill coefficients	2 (dimensionless)	fixed

243 **Table 1. Model parameters values**

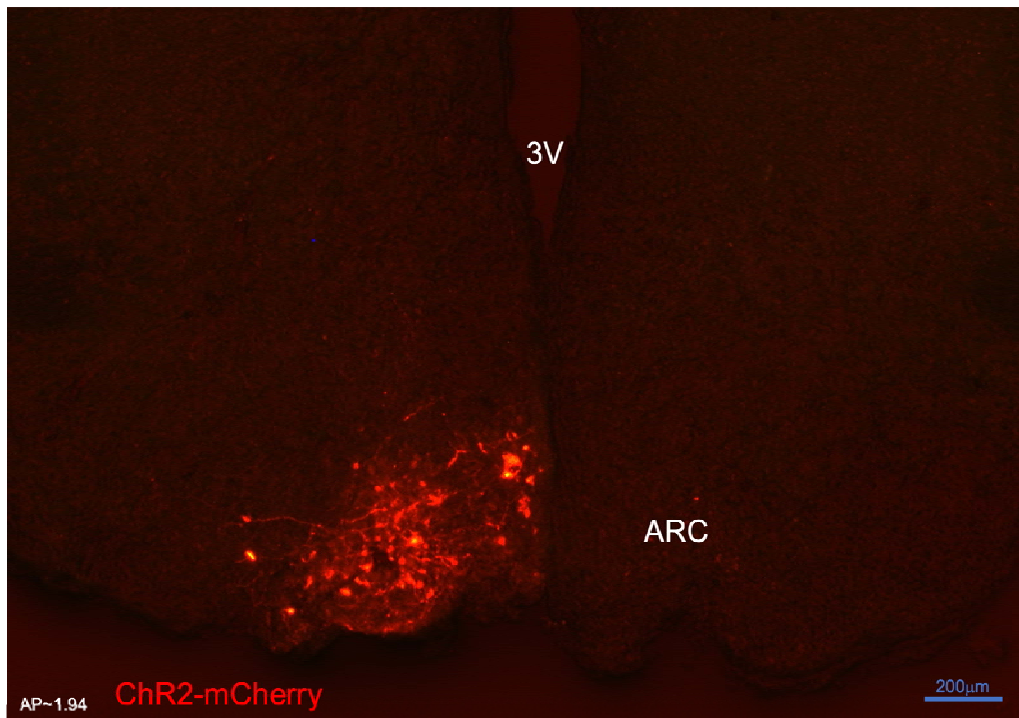
244 **Sensitivity & Principal Component Analysis**

245 We used principal component analysis to study the sensitivity of the system with respect to
246 changes in the four inferred parameters (Toni et al., 2009). We calculate the principal
247 components in the dataset (sampled posterior distribution) of the inferred parameter changes.
248 Principal component analysis produces a set of linearly uncorrelated eigen-parameters
249 explaining the variance of the inferred changes (in the sampled posterior distribution.) These
250 eigen-parameters are linear weighted combinations of the initial parameters. The eigen-
251 parameter explaining the least of the variance in the posterior distribution corresponds to the
252 stiffest parameter combination. That is small deviations from the inferred way these
253 parameters co-vary would lead to changes in the model behaviour that make it incompatible
254 with the data.

255 **Results**

256 **The dynamic response of the KNDy network to sustained, low-frequency optic** 257 **stimulation is estrous cycle dependent.**

258 Using optogenetics we perturbed the KNDy network to test whether and how sex steroids
259 modulate the system's dynamical response. ARC kisspeptin-expressing neurons were
260 transduced with a Cre-dependent adeno-associated virus (AAV9-EF1-*dflox*-hChR2-
261 (H134R)-mCherryWPRE-hGH) to express ChR2 (Fig. 1; see Materials and Methods) and
262 were optogenetically stimulated at the estrous and the diestrous phase of the cycle, measuring
263 LH pulse frequency as a readout. Sustained, low-frequency optic stimulation was used to
264 emulate elevated basal activity in ARC kisspeptin neurons or persistent stimulatory signals to
265 the KNDy population from other neuronal populations.



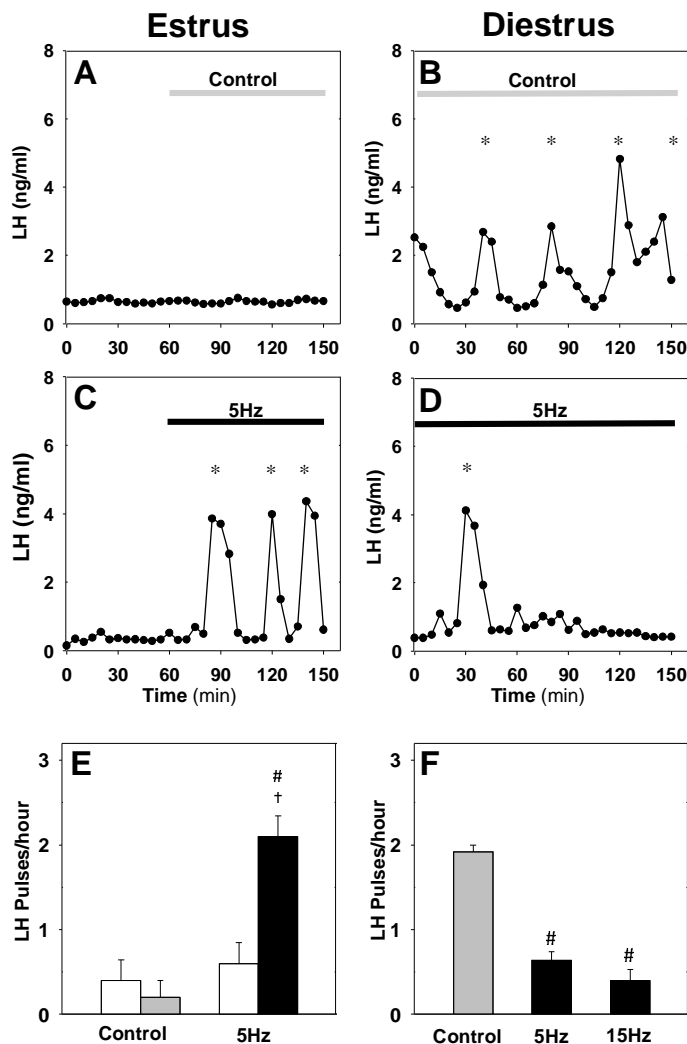
266

267 **Figure 1. Expression of arcuate nucleus (ARC) kisspeptin neurones with ChR2-mCherry in Kiss-Cre**
268 **mouse.** Coronal section showing red mCherry fluorescence positive neurons in the ARC which indicates ChR2
269 receptor expressing kisspeptin neurones, following unilateral injection of AAV9.EF1.dflox.hChR2(H134R)-
270 mCherry.WPRE.hGH into the ARC of Kiss-Cre mouse. Note the absence of mCherry fluorescence in the other
271 side of ARC. 3V, Third ventricle.

272

273 In estrous mice, we find that sustained optogenetic stimulation of ARC kisspeptin neurons at
274 5Hz immediately triggers robust LH pulses at a frequency of 2.10 ± 0.24 pulses/hour (Fig. 2
275 A,C&E), which is in agreement with our previous findings (Voliotis et al., 2019) and
276 highlights how pulsatile dynamics can emerge as a population phenomenon without the need
277 of a pulsatile activation signal (Strogatz, 2018). In diestrous mice, on the other hand,
278 optogenetic stimulation of ARC kisspeptin neurons at 5Hz leads to an apparent slowdown of
279 LH pulse frequency towards the end of the 1.5 h stimulation period (SI; Fig. S2). To
280 investigate the response in diestrous mice in greater detail we revised our experimental
281 protocol, removing the control period and extending the stimulation period to 2.5 h. With the
282 extended protocol we measure 0.64 ± 0.09 and 0.40 ± 0.13 LH pulses/hour under sustained
283 optic stimulation at 5 and 15Hz, respectively; these frequencies are significantly lower than
284 the LH pulse frequency we observe in control animals, which receive no optic stimulation
285 (Fig. 2 B,D&F). We note that we observe normal LH pulse frequencies in WT animals
286 receiving sustained optic stimulation for 2.5h (see SI; Fig. S1).

287 Our data illustrate how natural variation of ovarian steroids across the ovarian cycle leads to
 288 qualitative changes in the dynamical response of ARC kisspeptin neurons to optical
 289 stimulation. These changes are most probably driven by the effect that gonadal steroids have
 290 on the intrinsic electrophysiological properties of ARC kisspeptin neurons (Ruka et al., 2016)
 291 and the neuromodulator signalling capacity within the KNDy network (Vanacker et al.,
 292 2017).



293
 294 **Figure 2. Differential effect of optic stimulation of ARC kisspeptin neurons in estrous and diestrous Kiss-**
 295 **Cre mice.** (A-B) Representative examples showing LH secretion in response to no stimulation (grey bar) or
 296 sustained blue light (473 nm, 5-ms pulse width, black bar) activation of kisspeptin neurons at 5 Hz in estrous
 297 (C) and diestrous (D) mice. (E) Summary showing mean \pm SEM LH pulse frequency over the 60min control
 298 period (white bars) and over the subsequent stimulation period (black bar) in estrous mice. (F) Summary
 299 showing mean \pm SEM LH pulse frequency in the control (grey bar) and stimulated (black bars) diestrous mice.
 300 *Denote LH pulses. #P < 0.05 vs control; †P < 0.05 vs pre-stimulation; n = 5-6 per group.

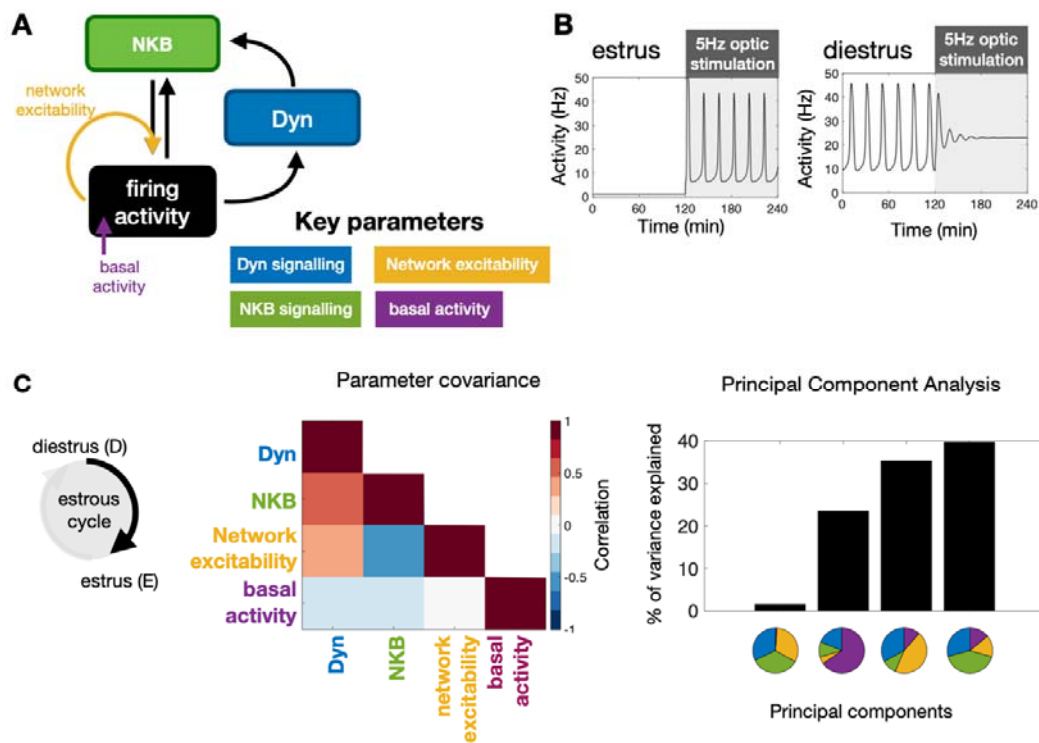
301 **A mathematical model predicts key mechanisms modulating the behaviour of the KNDy**
302 **pulse generator across the estrous cycle.**

303 Interrogating the KNDy network at different stages of the estrous cycle via optic stimulation
304 and measuring the effect on LH pulse frequency allows use of our mathematical model
305 (Voliotis et al., 2019) to understand how key system parameters change under gonadal steroid
306 control. The model describes the dynamical behaviour of ARC kisspeptin neurons using three
307 dynamical variables: representing the levels of Dyn, NKB and neuronal activity (Fig. 3 A).
308 We postulate that gonadal steroids could potentially modulate the behaviour of the KNDy
309 system across the cycle via acting on four key model parameters: (i) level of Dyn signalling,
310 (ii) level of NKB signalling, (iii) network excitability (i.e., propensity of neurons in the
311 population to transmit signals to one another), and (iv) basal neuronal activity.

312 Employing Bayesian inference techniques (see material and methods), we sample values for
313 these four parameters, which allow the model to replicate the mean LH frequency we observe
314 experimentally in estrus and diestrus mice with and without 5Hz optic stimulation (Fig. 2
315 E&F). Inspection of the dynamical behaviour of the model, using the identified diestrus
316 parameter values, reveals that in response to optic stimulation in diestrus pulsatile dynamics
317 could die out gradually (i.e, there is a transient period before activity shuts down; see Fig. 3 B
318 for an illustrative example), which is confirmed by the delayed inhibition of LH pulses we
319 observed experimentally in diestrus mice.

320 Next, we focus on how the four key parameters change between diestrus and estrus. We
321 measure the change in each parameter using the log-ratio of its estrous to diestrus value, and
322 calculate the covariance matrix of these log-ratios from our set of inferred parameter values.
323 We find a positive (linear) correlation between changes in Dyn and NKB signalling strength,
324 and negative (linear) correlation between changes in NKB signalling strength and network
325 excitability (Fig. 3 C). That is, the model predicts that NKB signalling strength and network
326 excitability are characterised by opposite (in direction) correlations during the transition from
327 diestrus to estrus (one decreasing the other increasing; we note the model predicts that both
328 combinations are possible), whereas NKB and Dyn signalling remain correlated in the same
329 direction (either increasing or decreasing; we note the model predicts that both combinations
330 are possible). Finally, we apply Principal Component Analysis to study the sensitivity of the
331 system with respect to changes in the four parameters (see Materials and Methods). We
332 calculate the principal components in dataset with the inferred parameter changes. Principal
333 components explaining small portions of the variance in the dataset (i.e., principal component

334 with the smallest eigenvalue) correspond to parameter combinations to which the system
 335 dynamics are most sensitive (stiff parameter combinations). These combinations are the most
 336 critical in terms of regulation as small deviations in how these parameters co-vary result in
 337 significant shifts in the system's dynamics. Interestingly, the principal component capturing
 338 the smallest share of the variance is comprised of the parameters controlling NKB signalling,
 339 Dyn signalling and network excitability in approximately equal portions, and therefore the
 340 model predicts that co-ordinated changes in these three parameters should be critical for the
 341 observed changes in system dynamics between diestrus and estrus. Interestingly, the second
 342 smallest principal component is largely determined by change in the basal activity parameter,
 343 suggesting that basal activity is another independent handle for modulating the system's
 344 dynamics. Taken together our theoretical findings suggest that co-ordinated changes in
 345 KNDy signalling as well as changes in KNDy basal activity may be crucial pathways of
 346 regulation across the reproductive cycle.



347
 348 **Figure 3. Model predictions on the key mechanisms modulating the behaviour of the KNDy pulse generator across the ovarian cycle.** (A) Schematic illustration of the coarse-grained model of the ARC KNDy
 349 population. The model comprises three dynamical variables representing the average levels of Dyn and NKB
 350 secreted by the population, and its average firing activity. We hypothesise that four key parameters modulate the
 351 behaviour of the system across the ovarian cycle: (i) Dyn signalling strength; (ii) NKB signalling strength; (iii)
 352 network excitability and (iv) basal neuronal activity. Estimates for the four parameters in estrus and diestrus are
 353

354 inferred from LH pulse frequency data in estrus and diestrus animals; with or without 5Hz optic stimulation
355 (Fig. 2 E&F) (B) System response to low frequency stimulation during estrus and diestrus, using the maximum
356 a-posteriori estimate of the parameter values inferred from the frequency data. (C) Analysis of parameter
357 changes across the cycle. For each of the four parameter (θ^i ; $i = 1,2,3,4$) the diestrus-to-estrus change is defined
358 as the log-ratio between the corresponding parameter values, i.e., $\log_{10} \frac{\theta^i_{\text{estrus}}}{\theta^i_{\text{diestrus}}}$. Normalised covariance
359 (correlation) matrix of parameter changes reveals negative correlation between changes in NKB signalling
360 strength and network excitability, and positive correlation between Dyn signalling strength and both NKB
361 signalling. Eigen-parameters are visualised as pie charts. The eigen-parameter explaining the least of the
362 variance in the posterior distribution corresponds to the stiffest parameter combination to which the system is
363 most sensitive.

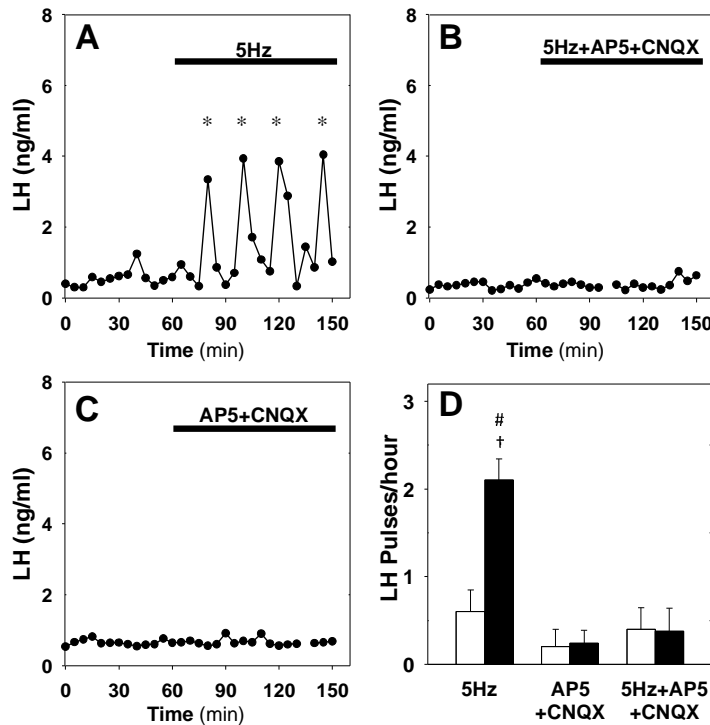
364 **Glutamatergic transmission in the KNDy population is critical for LH pulsatility**

365 Since KNDy neurons are primarily glutamatergic (Cravo et al., 2011; Nestor et al., 2016; Qiu
366 et al., 2016; Qiu et al., 2018) and synapse to one another (Yip et al., 2015; Qiu et al., 2016)
367 we hypothesise that glutamate transmission is a key driver of excitability within the KNDy
368 network. Hence to better understand how network excitability affects the dynamic behaviour
369 of the system across the ovarian cycle as the model predicts we disrupt signalling via
370 glutamate receptors and quantify the impact of this disruption on LH pulsatility.

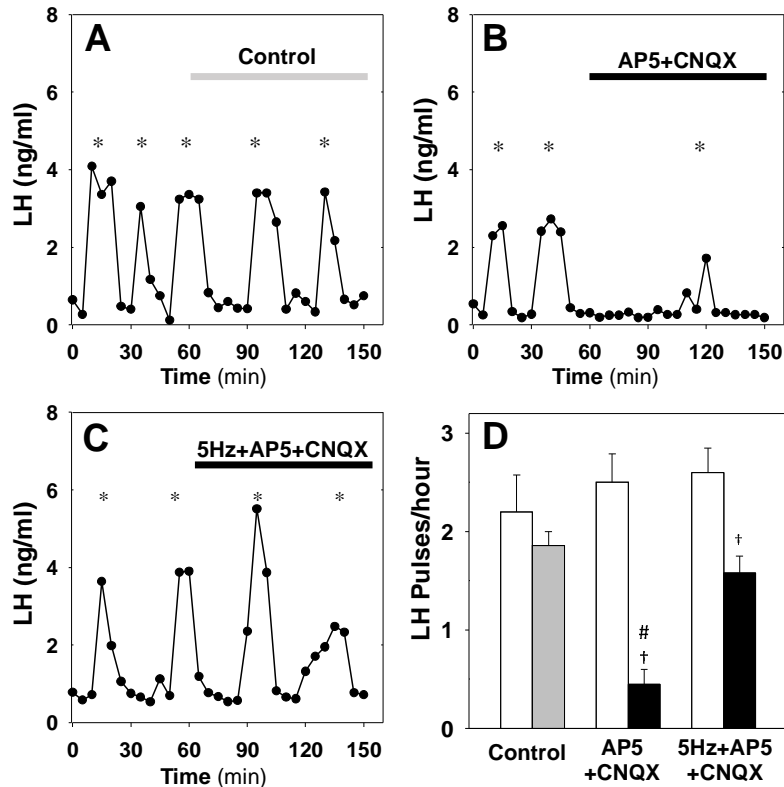
371 First, using Kiss-Cre estrous mice we test whether glutamatergic transmission is necessary
372 for the optogenetic induction of LH pulses. We drive the ARC kisspeptin population using
373 sustained, low-frequency optic stimulation (5 Hz) in the presence of the combined NMDA
374 and AMPA receptor antagonists (AP5 and CNQX, respectively). We find that blocking
375 signalling via glutamate receptors inhibits the capacity of optic stimulation to generate and
376 sustain pulsatile LH secretion (Fig. 4 A,B&D). The combined AP5 and CNQX in the absence
377 of optic stimulation had no effect (Fig. 4 C&D).

378 Next, we test whether glutamatergic transmission is critical for the endogenous LH pulses
379 observed in diestrus. Treatment of diestrous mice with the combined NMDA and AMPA
380 receptor antagonists resulted in a significant reduction of LH pulse frequency from $2.50 \pm$
381 0.29 to 0.45 ± 0.15 pulses/hour (Fig. 5 B&D), confirming that the glutamatergic transmission
382 is indeed critical for pulsatility. Moreover, combining NMDA and AMPA receptor antagonist
383 treatment with low frequency optic stimulation (5 Hz) partially restored LH pulsatility to 1.58
384 ± 0.17 pulses/hour (Fig. 5 C&D), suggesting low glutamatergic transmission within the
385 KNDy population or from upstream neuronal populations could be offset by other exogenous
386 inputs or elevated basal activity. This finding is in agreement with the model prediction that

387 basal activity and signalling between KNDy neurons are independent pathways of
388 modulating the system's dynamical behaviour.



389
390 **Figure 4. Effect of NMDA+AMPA receptor antagonists on pulsatile LH secretion in estrus.** Representative
391 examples showing LH secretion in estrous mice in response to optic stimulation (5Hz blue light, 473 nm, 5-ms
392 pulse width) (A) and optic stimulation combined with the NMDA+AMPA receptor antagonist (bolus ICV
393 injection [12 nmol AP5 + 5 nmol CNQX] over 5 min, followed by a continuous infusion [20 nmol AP5 and 10
394 nmol CNQX] for the remaining 90 min) treatment (B). NMDA+AMPA receptor antagonist alone had no effect
395 (C). (D) Summary showing mean \pm SEM LH pulse frequency over the 60min non-stimulatory period (white
396 bars) and over the subsequent 90 min stimulation period or appropriate non-stimulatory period in presence of
397 NMDA+AMPA receptor antagonist alone (black bar) in diestrous mice. *Denote LH pulses. $^{\dagger}P < 0.05$ vs pre-
398 stimulation. $^{\#}P < 0.05$ compared to antagonist treatment groups; n = 5-6 per group.



399

400 **Figure 5. Effect of NMDA+AMPA receptor antagonists on pulsatile LH secretion in diestrus.**

401 Representative examples showing pulsatile LH secretion in response to ICV administration of aCSF as control

402 (A), treatment with NMDA+AMPA receptor antagonists (AP5+CNQX: bolus ICV injection [12 nmol AP5 + 5

403 nmol CNQX] over 5 min, followed by a continuous infusion [20 nmol AP5 and 10 nmol CNQX] for the

404 remaining 90 min) (B) and combined NMDA/AMPA receptor antagonist treatment and sustained optic

405 stimulation (blue light 473 nm, 5-ms pulse width) at 5Hz (C). (D) Summary showing mean \pm SEM LH pulse

406 frequency over the 60min non-stimulatory period (white bars) and over the subsequent 90 min stimulation

407 period in control mice (grey bar) and mice receiving treatment (black bar). *Denote LH pulses. †P < 0.05 vs pre-

408 stimulation. #P < 0.05 compared to 5 Hz stimulation plus antagonist treatment and aCSF control groups; n = 5-6

409 per group.

410 Discussion

411 Using optogenetics we perturbed the GnRH pulse generator at different stages of the ovarian

412 cycle aiming to understand how gonadal steroids modulate key properties of the system.

413 Previous studies have shown how the pulsatile activity generated by the kisspeptin neuronal

414 network is modulated across the estrous cycle (Han et al., 2015; McQuillan et al., 2019). Our

415 data show that the stage of the cycle also has a profound effect on the dynamical response of

416 the kisspeptin population to sustained, low frequency optic stimulation. Such stimulation

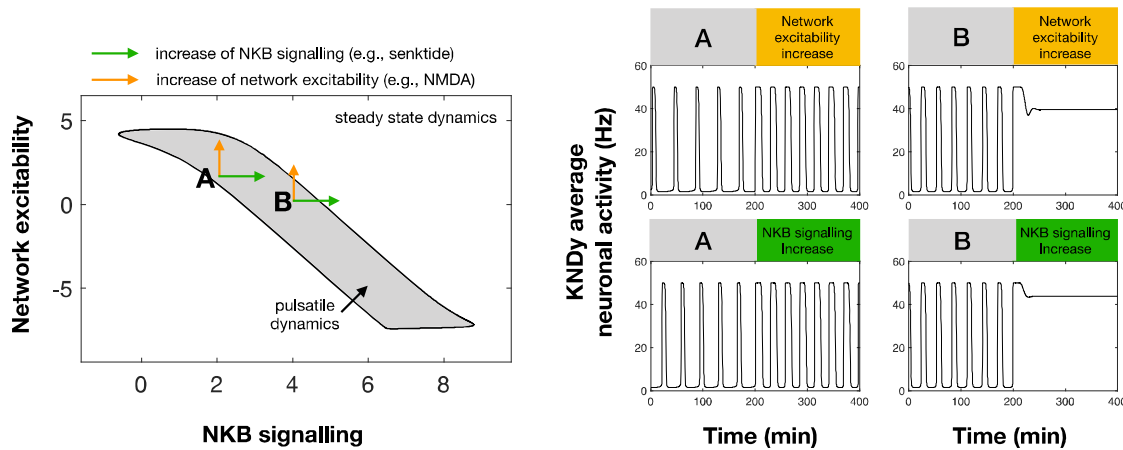
417 triggers acceleration of LH pulses during estrus and deceleration during diestrus. Previously,
418 our mathematical model of the KNDy network has predicted an upper and a lower bifurcation
419 point that determine the system's range of pulsatile behaviour as the system is driven
420 externally (Voliotis et al., 2019). Our data suggest that the gonadal state plays a critical role
421 in shifting these bifurcation points by modulating key parameters of the system. In particular,
422 during estrous the system is positioned below the lower bifurcation point and optogenetic
423 stimulation of ARC kisspeptin neurons at 5Hz move the system across the lower bifurcation
424 point leading to the sudden emergence of pulsatile behaviour. In contrast, during diestrus the
425 system is within the pulsatile regime and optogenetic stimulation of ARC kisspeptin neurons
426 at frequencies greater than 5Hz move the system across the upper bifurcation point and its
427 dynamics relax progressively from pulsatile to quiescent. Our data therefore highlight the
428 critical role of gonadal steroids in modulating the dynamical response of the KNDy network
429 to small changes in basal activity of ARC kisspeptin neurons or in how the population
430 processes external perturbations and afferent inputs.

431 Using our mathematical model of the system we gained insight into possible mechanisms via
432 which gonadal steroids modulate the dynamic behaviour of the GnRH pulse generator. Based
433 on the LH pulse frequency observed in estrous and diestrous animals under no optic
434 stimulation or with 5Hz optic stimulations, the model predicted that network excitability is an
435 important parameter of the system, which could be modulated at different stages of the
436 ovarian cycle. Importantly, KNDy network excitability is most probably co-regulated with
437 parameters controlling the strength of Dyn and NKB signalling as the system transitions
438 between the different phases of the ovarian cycle. In particular, our analysis suggests strong
439 negative correlation between changes in NKB signalling strength and changes in network
440 excitability and strong positive correlation in changes between NKB and Dyn signalling.
441 Interestingly these findings are in line with recent transcriptomic data showing that treatment
442 of ovariectomised mice with estradiol reduced expression of NKB and Dyn in KNDy
443 neurons, but increased expression of glutamate transporters (vGlut2), which lead to increased
444 glutamate neurotransmission and neuronal excitability in the population (Qiu et al., 2018).

445 The effect of cycle stage on the LH response to sustained optogenetic stimulation is
446 reminiscent of the well documented effect that gonadal steroids have on LH response to
447 various excitatory neurotransmitters and neuropeptides (e.g., NMDA). For instance,
448 investigations in the female monkey revealed an unexplained inhibition of LH in OVX

449 animals following treatment with NMDA, in contrast with the excitatory action of NMDA on
450 LH secretion in the presence of ovarian steroids (Reyes et al., 1990; Reyes et al., 1991).
451 Similar reversal of action on LH dynamics depending on the underlying ovarian steroid
452 milieu has been documented for various other neurotransmitters and NKB receptor agonists
453 (Kalra and Kalra, 1983; Scorticati et al., 2004). Our mathematical model supports that
454 ovarian steroids change key parameters of the KNDy network, which control the dynamic
455 behaviour of the system and its response to perturbations. As an illustration, Fig. 6 shows
456 how the dynamic behaviour of the model depends on network excitability and NKB
457 signalling. Since these parameters are governed by gonadal steroids (Qiu et al., 2018; Wang
458 et al., 2018), it is expected that the underlying steroid milieu will also modulate the effect of
459 perturbations on the dynamics of the system. For instance, the effect of stimulating NKB
460 signalling (e.g., via administration of NK3 receptor agonists) or network excitability (e.g., via
461 NMDA administration) could result in inhibition of the pulse generator if the system is
462 already located closer to the right boundary of the pulsatile dynamics region (e.g., point B in
463 Fig. 6). Such points correspond to states with high pulse generator activity similar to pulse
464 generator dynamics observed in many animal models after gonadectomy (Reyes et al., 1990;
465 Kinsey-Jones et al., 2012). In contrast, similar perturbations but from a different point in the
466 parameter space, lying closer to the left edge of the pulsatile region (e.g., point A in Fig. 6),
467 could result in stimulation of the pulse generator (higher frequency). This illustrative example
468 also highlights that the effect of gonadal steroids on the response of the pulse generator to
469 perturbations is continuous rather than binary, that is, the behaviour of the pulse generator is
470 modulated by the actual continuous levels of gonadal steroids rather than their mere presence
471 of absence. Therefore, the underlying steroid levels could explain seemingly incompatible
472 findings regarding the effect of NKB receptor agonism on LH secretion: ranging from
473 stimulation (Navarro et al., 2011) or inhibition (Sandoval-Guzman and Rance, 2004; Kinsey-
474 Jones et al., 2012) to no effects (Navarro et al., 2009) in rodents.

475



476
477
478
479
480
481
482

Figure 6. Differential effect of perturbations on the dynamics of the pulse generator. Two-parameter (NKB signalling and Network excitability) bifurcation diagram showing the region in the parameter space for which the system exhibits pulsatile dynamics (grey area). Two points (denoted by A and B) illustrate how an increase in NKB signalling or network excitability could have a differential effect on the dynamics of the system. For point A an increase in network excitability or NKB signalling could lead to an increase in the frequency and width of pulses. However, for point B a similar increase leads to pulse inhibition and steady state system dynamics.

483 Based on our model predictions regarding the importance of network excitability, we set out
484 to uncover the role of this parameter on the dynamic response of the network in-vivo. We
485 hypothesised that network excitability should critically depend on the levels of glutamate
486 signalling as ARC kisspeptin neurons are known to be interconnected (Yip et al., 2015; Qiu
487 et al., 2016) and communicate via glutamate (Cravo et al., 2011; Qiu et al., 2011; Nestor et
488 al., 2016; Qiu et al., 2016). Further evidence that estradiol regulates KNDy neuronal
489 excitability (Qiu et al., 2018) and that cycle stage regulates spontaneous glutamatergic
490 activity of KNDy neurons (Wang and Moenter, 2020) supports the model prediction that
491 network excitability is a critical network property regulated by gonadal steroids. Therefore, to
492 further test this prediction in-vivo we used glutamate receptor (NMDA and AMPA)
493 antagonists to inhibit excitability in the KNDy network. In diestrus animals blocking
494 glutamate receptors (NMDA and AMPA) inhibited LH pulses that were then rescued via low
495 frequency optogenetic stimulation of kisspeptin neurons. Furthermore, in estrus animals,
496 NMDA and AMPA receptor antagonism inhibited the induction of LH pulses via optic
497 stimulation. These experimental findings highlight the complex fine-balanced mechanisms
498 underlying pulse generation by the KNDy network. In particular, limited glutamatergic
499 signalling within the KNDy population blocks LH pulsatility but this can be mitigated by
500 elevated basal neuronal activity. Similarly, increased basal neuronal activity can induce pulse
501 generation but this effect can be negated by decreased glutamatergic signalling within the
502 neuronal population. . There is a caveat, however, as the glutamate receptor antagonists were
503 given by intracerebroventricular injection and this raises the possibility of additionally

504 interfering with glutamatergic transmission from afferent populations. However, to the best
505 of our knowledge there is no clear evidence of such glutamatergic inputs into the KNDy
506 population. Furthermore, blocking possible exogenous glutamatergic inputs does not
507 invalidate our model, but further supports one of its key predictions that basal activation of
508 KNDy neurons is a critical pathway for modulating the dynamics of the pulse generator.
509 Overall, our model predicts that pulse generation is an emergent property of the KNDy
510 network depending both on single neuron properties such as basal activity and exogeneous
511 activation but also on how the neurons signal and communicate with each other. Our results
512 support this idea, highlighting the critical role of glutamate in enabling the population to
513 pulse in synchrony.

514

515 **Acknowledgments:** The authors gratefully acknowledge the financial support of the EPSRC
516 via grant EP/N014391/1 (KTA and MV), and BBSRC via grants BB/S000550/1 and
517 BB/S001255/1 (KTA, KOB, MV, XFL).

518 **References**

519

- 520 Arias P, Jarry H, Leonhardt S, Moguilevsky JA, Wuttke W (1993) Estradiol modulates the
521 LH release response to N-methyl-D-aspartate in adult female rats: studies on
522 hypothalamic luteinizing hormone-releasing hormone and neurotransmitter release.
523 *Neuroendocrinology* 57:710-715.
- 524 Bonavera JJ, Sahu A, Kalra SP, Kalra PS (1994) The hypothalamic peptides, beta-endorphin,
525 neuropeptide K and interleukin-1 beta, and the opiate morphine, enhance the
526 excitatory amino acid-induced LH release under the influence of gonadal steroids. *J*
527 *Neuroendocrinol* 6:557-564.
- 528 Brann DW, Mahesh VB (1992) Excitatory amino acid regulation of gonadotropin secretion:
529 modulation by steroid hormones. *J Steroid Biochem Mol Biol* 41:847-850.
- 530 Christian CA, Moenter SM (2010) The neurobiology of preovulatory and estradiol-induced
531 gonadotropin-releasing hormone surges. *Endocr Rev* 31:544-577.
- 532 Cravo RM, Margatho LO, Osborne-Lawrence S, Donato J, Jr., Atkin S, Bookout AL,
533 Rovinsky S, Frazao R, Lee CE, Gautron L, Zigman JM, Elias CF (2011)
534 Characterization of Kiss1 neurons using transgenic mouse models. *Neuroscience*
535 173:37-56.
- 536 Czieselsky K, Prescott M, Porteous R, Campos P, Clarkson J, Steyn FJ, Campbell RE,
537 Herbison AE (2016) Pulse and Surge Profiles of Luteinizing Hormone Secretion in
538 the Mouse. *Endocrinology* 157:4794-4802.
- 539 Dutton A, Dyball RE (1979) Phasic firing enhances vasopressin release from the rat
540 neurohypophysis. *J Physiol* 290:433-440.
- 541 Goodman RL, Holaskova I, Nestor CC, Connors JM, Billings HJ, Valent M, Lehman MN,
542 Hileman SM (2011) Evidence that the arcuate nucleus is an important site of
543 progesterone negative feedback in the ewe. *Endocrinology* 152:3451-3460.
- 544 Han SY, McLennan T, Czieselsky K, Herbison AE (2015) Selective optogenetic activation of
545 arcuate kisspeptin neurons generates pulsatile luteinizing hormone secretion. *Proc*
546 *Natl Acad Sci U S A* 112:13109-13114.

- 547 Kalra SP, Kalra PS (1983) Neural regulation of luteinizing hormone secretion in the rat.
548 *Endocr Rev* 4:311-351.
- 549 Kelly MJ, Zhang C, Qiu J, Ronnekleiv OK (2013) Pacemaking kisspeptin neurons. *Exp*
550 *Physiol* 98:1535-1543.
- 551 Kinsey-Jones JS, Grachev P, Li XF, Lin YS, Milligan SR, Lightman SL, O'Byrne KT (2012)
552 The inhibitory effects of neurokinin B on GnRH pulse generator frequency in the
553 female rat. *Endocrinology* 153:307-315.
- 554 Lass G, Li XF, de Burgh RA, He W, Kang Y, Hwa-Yeo S, Sinnott-Smith LC, Manchishi SM,
555 Colledge WH, Lightman SL, O'Byrne KT (2020) Optogenetic stimulation of
556 kisspeptin neurones within the posterodorsal medial amygdala increases luteinising
557 hormone pulse frequency in female mice. *J Neuroendocrinol* 32:e12823.
- 558 McQuillan HJ, Han SY, Cheong I, Herbison AE (2019) GnRH Pulse Generator Activity
559 Across the Estrous Cycle of Female Mice. *Endocrinology* 160:1480-1491.
- 560 Moore AM, Coolen LM, Porter DT, Goodman RL, Lehman MN (2018) KNDy Cells
561 Revisited. *Endocrinology* 159:3219-3234.
- 562 Navarro VM, Gottsch ML, Chavkin C, Okamura H, Clifton DK, Steiner RA (2009)
563 Regulation of gonadotropin-releasing hormone secretion by
564 kisspeptin/dynorphin/neurokinin B neurons in the arcuate nucleus of the mouse. *J*
565 *Neurosci* 29:11859-11866.
- 566 Navarro VM, Castellano JM, McConkey SM, Pineda R, Ruiz-Pino F, Pinilla L, Clifton DK,
567 Tena-Sempere M, Steiner RA (2011) Interactions between kisspeptin and neurokinin
568 B in the control of GnRH secretion in the female rat. *Am J Physiol Endocrinol Metab*
569 300:E202-210.
- 570 Nestor CC, Qiu J, Padilla SL, Zhang C, Bosch MA, Fan W, Aicher SA, Palmiter RD,
571 Ronnekleiv OK, Kelly MJ (2016) Optogenetic Stimulation of Arcuate Nucleus Kiss1
572 Neurons Reveals a Steroid-Dependent Glutamatergic Input to POMC and AgRP
573 Neurons in Male Mice. *Mol Endocrinol* 30:630-644.
- 574 Paxinos G, Franklin KBJ (2004) *The Mouse Brain in Stereotaxic Coordinates*, 2nd Edition:
575 Elsevier Academic Press.
- 576 Qiu J, Fang Y, Bosch MA, Ronnekleiv OK, Kelly MJ (2011) Guinea pig kisspeptin neurons
577 are depolarized by leptin via activation of TRPC channels. *Endocrinology* 152:1503-
578 1514.
- 579 Qiu J, Nestor CC, Zhang C, Padilla SL, Palmiter RD, Kelly MJ, Ronnekleiv OK (2016)
580 High-frequency stimulation-induced peptide release synchronizes arcuate kisspeptin
581 neurons and excites GnRH neurons. *Elife* 5:e16246-e16246.
- 582 Qiu J, Rivera HM, Bosch MA, Padilla SL, Stincic TL, Palmiter RD, Kelly MJ, Ronnekleiv
583 OK (2018) Estrogenic-dependent glutamatergic neurotransmission from kisspeptin
584 neurons governs feeding circuits in females. *Elife* 7.
- 585 Reyes A, Luckhaus J, Ferin M (1990) Unexpected inhibitory action of N-methyl-D,L-
586 aspartate or luteinizing hormone release in adult ovariectomized rhesus monkeys: a
587 role of the hypothalamic-adrenal axis. *Endocrinology* 127:724-729.
- 588 Reyes A, Xia LN, Ferin M (1991) Modulation of the effects of N-methyl-D,L-aspartate on
589 luteinizing hormone by the ovarian steroids in the adult rhesus monkey.
590 *Neuroendocrinology* 54:405-411.
- 591 Ruka KA, Burger LL, Moenter SM (2016) Both Estrogen and Androgen Modify the
592 Response to Activation of Neurokinin-3 and kappa-Opioid Receptors in Arcuate
593 Kisspeptin Neurons From Male Mice. *Endocrinology* 157:752-763.
- 594 Sandoval-Guzman T, Rance NE (2004) Central injection of senktide, an NK3 receptor
595 agonist, or neuropeptide Y inhibits LH secretion and induces different patterns of Fos
596 expression in the rat hypothalamus. *Brain Res* 1026:307-312.

- 597 Scorticati C, Fernandez-Solari J, De Laurentiis A, Mohn C, Prestifilippo JP, Lasaga M,
598 Seilicovich A, Billi S, Franchi A, McCann SM, Rettori V (2004) The inhibitory effect
599 of anandamide on luteinizing hormone-releasing hormone secretion is reversed by
600 estrogen. *Proc Natl Acad Sci U S A* 101:11891-11896.
- 601 Seabrook GR, Bowery BJ, Hill RG (1995) Pharmacology of tachykinin receptors on
602 neurones in the ventral tegmental area of rat brain slices. *Eur J Pharmacol* 273:113-
603 119.
- 604 Steyn FJ, Wan Y, Clarkson J, Veldhuis JD, Herbison AE, Chen C (2013) Development of a
605 methodology for and assessment of pulsatile luteinizing hormone secretion in juvenile
606 and adult male mice. *Endocrinology* 154:4939-4945.
- 607 Strogatz SH (2018) *Nonlinear dynamics and chaos with student solutions manual: With*
608 *applications to physics, biology, chemistry, and engineering: CRC press.*
- 609 Toni T, Welch D, Strelkowa N, Ipsen A, Stumpf MP (2009) Approximate Bayesian
610 computation scheme for parameter inference and model selection in dynamical
611 systems. *J R Soc Interface* 6:187-202.
- 612 Vanacker C, Moya MR, DeFazio RA, Johnson ML, Moenter SM (2017) Long-Term
613 Recordings of Arcuate Nucleus Kisspeptin Neurons Reveal Patterned Activity That Is
614 Modulated by Gonadal Steroids in Male Mice. *Endocrinology* 158:3553-3564.
- 615 Vidal A, Zhang Q, Medigue C, Fabre S, Clement F (2012) DynPeak: an algorithm for pulse
616 detection and frequency analysis in hormonal time series. *PLoS One* 7:e39001.
- 617 Voliotis M, Li XF, De Burgh R, Lass G, Lightman SL, O'Byrne KT, Tsaneva-Atanasova K
618 (2019) The Origin of GnRH Pulse Generation: An Integrative Mathematical-
619 Experimental Approach. *J Neurosci* 39:9738-9747.
- 620 Wang L, Moenter SM (2020) Differential Roles of Hypothalamic AVPV and Arcuate
621 Kisspeptin Neurons in Estradiol Feedback Regulation of Female Reproduction.
622 *Neuroendocrinology* 110:172-184.
- 623 Wang L, Burger LL, Greenwald-Yarnell ML, Myers MG, Jr., Moenter SM (2018)
624 Glutamatergic Transmission to Hypothalamic Kisspeptin Neurons Is Differentially
625 Regulated by Estradiol through Estrogen Receptor alpha in Adult Female Mice. *J*
626 *Neurosci* 38:1061-1072.
- 627 Yasuda K, Raynor K, Kong H, Breder CD, Takeda J, Reisine T, Bell GI (1993) Cloning and
628 functional comparison of kappa and delta opioid receptors from mouse brain. *Proc*
629 *Natl Acad Sci U S A* 90:6736-6740.
- 630 Yeo SH, Kyle V, Morris PG, Jackman S, Sinnett-Smith LC, Schacker M, Chen C, Colledge
631 WH (2016) Visualisation of Kiss1 Neurone Distribution Using a Kiss1-CRE
632 Transgenic Mouse. *J Neuroendocrinol* 28.
- 633 Yip SH, Boehm U, Herbison AE, Campbell RE (2015) Conditional Viral Tract Tracing
634 Delineates the Projections of the Distinct Kisspeptin Neuron Populations to
635 Gonadotropin-Releasing Hormone (GnRH) Neurons in the Mouse. *Endocrinology*
636 156:2582-2594.
637